

Electromagnetic images of a strike-slip fault: The Tintina fault—Northern Canadian

Juanjo Ledo and Alan G. Jones

Geological Survey of Canada, Ottawa, Ontario, Canada

Ian J. Ferguson

Geological Sciences, University of Manitoba, Winnipeg Manitoba, Canada

Received 8 May 2001; revised 24 September 2001; accepted 25 October 2001; published 24 April 2002.

[1] Wideband magnetotelluric (MT) data were acquired along three profiles crossing the strike-slip Tintina Fault in northwestern Canada. The MT responses obtained exhibit remarkable similarity from all three profiles, implying similar two-dimensional (2-D) electromagnetic behavior of the fault zone over a strike length of at least 350 km. Analyses of the MT responses for dimensionality corroborate the validity of assuming regional 2-D structures in interpretation. Several high conductivity anomalies at different depth scales are present in the models obtained, and we suggest that both the shallow structures and the deep crustal scale anomalies are caused by electronic conduction mechanisms in interconnected mineralized zones. Intriguingly, the middle and lower crust beneath the surface expression of the Tintina Fault is highly resistive, in contrast to some other large-scale strike-slip faults. This implies that fault zone processes that result in interconnected conducting phases are not generic in nature but are controlled by local conditions. *INDEX TERMS:* 0905 Exploration Geophysics: Continental structures (8109, 8110); 8102 Tectonophysics: Continental contractional orogenic belts; 8110 Tectonophysics: Continental tectonics—general (0905)

1. Introduction

[2] The northern Cordillera of western North America comprises a region of oceanic and island-arc terranes accreted to North America since the Neoproterozoic, with most of this westward growth occurring in the last 200 Ma [Coney *et al.*, 1980]. Within this collage the most dominant feature (Figure 1) is the northern Rocky Mountain Trench—Tintina strike-slip fault (TTF), a 2,000-km-long transcurrent fault with an estimated 450-km or more of late Cretaceous to Oligocene dextral movement north of 60°N [Tempelman-Kluit, 1979]. To the south, the displacement diminishes to ca. 150 km [Monger *et al.*, 1994] and only occurs on faults younger than much of the motion on the TTF (e.g., Fraser Fault). At the surface, rocks to the northeast of the TTF are predominantly sedimentary and represent the ancient North American margin. Rocks to the southwest of the TTF are mostly young, mainly igneous and metamorphic, and constitute numerous accreted terranes. There is little seismic activity along the trace of the TTF in northern B.C. and Yukon [Lowe *et al.*, 1994]; west of the fault, activity is moderate with small-magnitude earthquakes ($M < 4$) whereas to the east there is a pronounced quiescent zone. Thus, the TTF appears to separate crust with different physical properties.

[3] Preliminary interpretation of deep seismic reflection data across the TTF by Cook *et al.* [2001] suggests a crustal penetrating

break with a complex geometry. This crustal difference may extend into the upper mantle: A recent study of potential-field data [Geiger and Cook, 2001] suggests that north of 60°N the TTF penetrates much of the lithosphere. Also, from an isotopic study of recent alkaline lavas, Abraham *et al.* [2001] concluded that the Tintina Fault in the Yukon and northern British Columbia is a high angle feature that penetrates the upper mantle to at least 70+ km and separates two distinct sub-continental lithospheric mantle roots.

[4] The TTF is being studied as part of Lithoprobe's Slave-Northern Cordillera Lithospheric Evolution (SNORCLE) transect [Clowes *et al.*, 1992], and one of the principle objectives of the SNORCLE transect was to determine the lithospheric geometry and internal properties of the TTF. To address this question, an electromagnetic survey, using the natural-source magnetotelluric (MT) technique, was designed with three fault-crossing profiles. MT has been used successfully to investigate major fault systems, both active and fossil, around the world [Stanley *et al.*, 1990; Jones *et al.*, 1992; Mackie *et al.*, 1997; Unsworth *et al.*, 1997; Ingham and Brown, 1998; Unsworth *et al.*, 1999; Wu *et al.*, 2001]. In this paper we present results from modeling and initial interpretation of the three MT profiles crossing the TTF.

2. Magnetotelluric Data

[5] Data along three regional magnetotelluric (MT) profiles crossing the TTF at different locations (Figure 1) were acquired to determine the subsurface geometry and character of the fault. The period range of the estimated MT and geomagnetic transfer function responses is from 0.0014 s to 10,000 s; we analyse the data in the range 0.0014 s to 1,000 s and model the responses between 0.01 s and 1,000 s to focus on the spatially-unaliased crustal features.

[6] Oppositely-directed induction vectors on the three profiles (Figure 2) suggest the presence of currents flowing in conducting structures at mid-crustal depths southwest of the fault zone surface trace. To determine the geoelectric strike of the regional structures and estimate the regional two-dimensional (2D) impedance tensors we applied the distortion decomposition method of Groom and Bailey [1989], as extended by McNeice and Jones [2001], with an error floor of 5% on the impedance tensor components. The best-fit average regional strikes (-50° for profile 300 and -45° for profiles 200 and 400) are consistent with the trends of the major outcropping geological structures. The regional 2-D MT impedances describing currents flowing along the TTF are called the transverse-electric (TE) mode responses, and the impedances describing currents crossing the TTF are called the transverse-magnetic (TM) mode responses. Figure 3 shows the distortion-corrected TE and TM apparent resistivity data for six selected sites close to the surface trace of the fault; two from each profile (their locations are marked by "a" and "b" in Figure 3). The

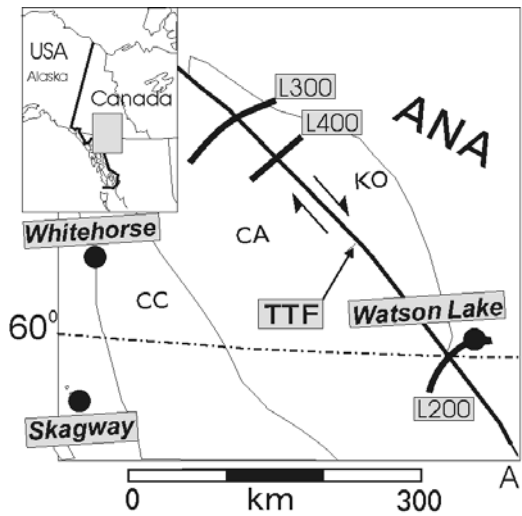


Figure 1. Map of western North America; shaded area in inset corresponds to the location of Figure 1a. (a) Geological sketch of southern Yukon and northern B.C. showing the locations of the MT profiles. TTF: Tintina Fault; ANA: Ancestral North America; Accreted terranes: CA: Cassiar terrane, CC: Cache Creek terrane, KO: Kootenay terrane; MT profiles, L200: profile 200, L300: profile 300, L400: profile 400.

similarity in response between the data is striking, in spite of the large along-strike separation between the sites.

3. 2-D Inversion

[7] For each profile 2-D regularized inversions of the TE and TM apparent resistivities and phases were undertaken using the algorithm of *Rodi and Mackie* [2001]. This algorithm searches simultaneously for the model with the lowest overall RMS misfit and the smallest lateral and vertical conductivity gradients. On average, we fitted the logarithm of the apparent resistivity data to

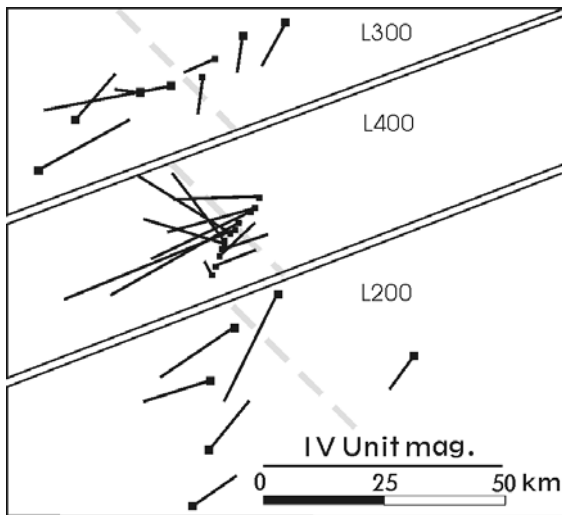


Figure 2. Real (reversed) induction vectors at a period of 30 s, the vectors point perpendicular to current concentrations. Discontinuous line represents the surface trace of the TTF.

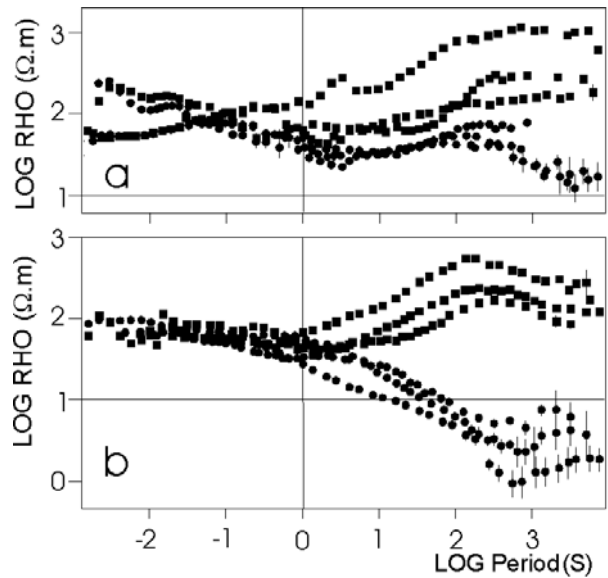


Figure 3. Apparent resistivity responses from six sites, two from each profile. Of the site pairs, one was on the west side of the fault (upper diagram), labeled (a) in Figure 4, and one was on the east side of the fault (lower diagram), labeled (b) in Figure 4. Squares: TM-mode data; circles: TE-mode data.

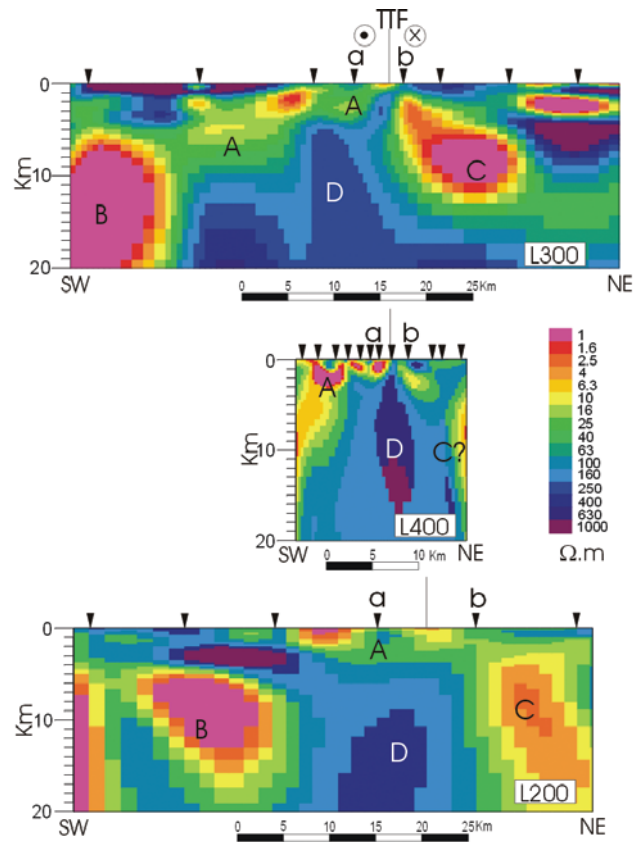


Figure 4. Two-dimensional resistivity models obtained by inversion of both the TE- and TM-mode resistivities and phases. Inverted triangles show the position of the MT sites. The TTF lies between points a and b which correspond to the location of sites presented in Figure 3.

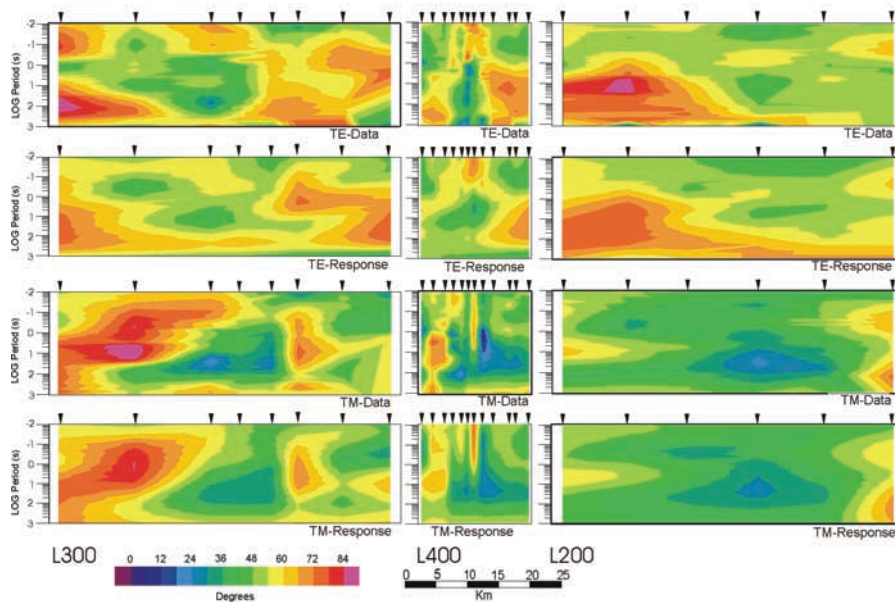


Figure 5. Comparison of phases from both TE- and TM-mode for the data (top) and model responses (bottom) for each profile. Inverted triangles show the position of the MT sites.

within 5% and the phases to within 1.4° . Neither structural features nor conductivity discontinuities were imposed a priori, and the initial model for all inversions was a $100 \Omega \cdot \text{m}$ uniform half space. Although the geomagnetic transfer functions (a component of the TE mode response) were not used during the inversion procedure, the final models obtained reproduced their main features. These final models are shown in Figures 4 and 5 compares the observed and modeled phases in pseudosection format. The worst fit is found for the TE mode in the central part of the regional profiles and is likely due to 3D effects [e.g., Wannamaker et al., 1984] not removed during distortion decomposition. The similarity in conductivity structures - in terms of their geometries and conductivity values - between the three models is apparent. All three models exhibit several high conductivity structures ($\sim 1-10 \Omega \cdot \text{m}$) with subvertical structures below the surface trace of the TTF up to 5 km depth (labeled A in Figure 4) that can be spatially associated with the fault system. At deeper levels (below 5 km) to the southwest a significant conductivity structure ($\sim 1 \Omega \cdot \text{m}$) is present (labeled B in Figure 4). Along profile 300, the southwestern extension of this structure is defined by additional data located further to the southwest (not shown here), confirming that the structure is not an artifact introduced by the inversion algorithm. Tests demonstrate that the MT data cannot discriminate whether anomalies A and B are connected or whether they are independent structures. To the northeast a second mid-crustal conductive structure is imaged (labeled C in Figure 4), although the lack of sites to the NE along profile 400 permit only its identification by the end site along that profile. Finally, another striking common feature of the three models is the occurrence of a highly resistive zone at deep crustal levels below the surface trace of the TTF (labeled D in Figure 4). This resistive zone is associated with the fault itself and its existence is a constraint to the possible geological models explaining the fault.

4. Discussion

[8] The high conductivity anomalies located near the surface trace of the TTF system (labeled A in Figure 4) are most likely associated with the presence of conducting minerals or, alternatively and less likely, (from fluid escape arguments) with saline fluids in fractures. The study area contains important mineral

deposits (Au, Cu, Pb-Zn, and VMS deposits) that are likely Mesozoic intrusion-related [Yukon MINFILE, 1997]. The strike-slip faults provide a conduit for relatively rapid fluid ascent in the formation of these deposits [Nesbitt and Muehlenbachs, 1988]. Stable isotope analysis of vein carbonate from the Ketz river mine mineral deposits [Staveley et al., 1991], close to the southwest end of profile 400, indicates a dominance of meteoritic water in the hydrothermal fluids, although some data also suggest the presence of magmatic fluids. These Mesozoic fluids were highly mobile, and the transport and precipitation of metals likely caused the shallow high conductivity anomalies observed.

[9] The deeper conductivity structures (labeled B and C in Figure 4) can only be explained in terms of conducting minerals because of the high conductivity values observed. Given the many carbon-rich rocks units in this part of the Cordillera, the presence of interconnected graphite is a ready explanation for these values. High conductivity rocks to depths greater than 20 km in the Denali fault [Stanley et al., 1990], another strike-slip fault in the Northern Canadian Cordillera, have also been associated with the presence of interconnected graphite films [Mathez et al., 1995]. This thesis was recently supported by Aleinikoff et al. [2000] in their interpretation of Pb, Sr, Nd and O isotopic data of Mesozoic and younger granitic rocks close to the Denali fault. To obtain such low resistivity values with saline fluids would require large volumes of fluid that would be gravitationally-unstable. Also, there is no geological or geophysical evidence to support a fluid interpretation. Perhaps the most significant feature in the conductivity models obtained is not the conductive structures, but rather the lack of one; namely the presence of a high resistivity structure at deep crustal levels directly below the surface trace of the TTF system (labeled D in Figure 4). This observation is consistent with the regional MT study of the San Andreas Fault at Carrizo Plain by Mackie et al. [1997] that also suggested a high resistivity zone at mid-crustal depths. Contrarily, an MT study of the Fraser Fault (FF) [Jones et al., 1992], which was active subsequently to the TTF and is thought to be part of the same fault system [Price and Carmichael, 1986], revealed that the FF penetrates the entire crust with a subvertical geometry and exhibits enhanced conductivity at mid-crustal depths. For the FF the cause of the enhanced conductivity was thought to be graphite precipitated from emerging, deeply penetrating meteoric waters [Jones et al., 1992].

[10] Snyder and Roberts [2001] obtained a high resolution reflection section across the TTF along profile 300, but within the uppermost ten kilometers existing reflectors are weak. Those observed are consistent with a crustal-scale flower structure. The crustal scale reflection section shows a major disruption of lower crustal reflectors and suggests the fault cuts the entire crust. The seismic reflection profile 200 [Cook et al., 2001] also indicates a break in reflectivity at lower crustal levels. The velocity models obtained from seismic refraction experiments along profile 200 close to the TTF zone [Weldford et al., 2001] show a distinct change across the TTF in the mid-crust. At lower crustal depths the wide-angle data are thought not to suggest prominent changes in the velocity structure across the fault. In summary, both reflection and refraction data reveal a 20–30 km wide transition zone in the middle to lower crust in which there are significant changes in seismic structure. This transition zone correlates well with the resistive structure of the MT models (labeled D in Figure 4). In contrast, the seismic reflection data of the FF [Varsek et al., 1993] reveals a middle crust that is characterized by horizontal reflections that are quasi-continuous beneath the FF. Therefore, both the electrical conductivities and the reflection patterns of these two strike-slip faults are different. The absence of a conducting zone at mid-crustal levels in the TTF may be attributed to the absence of circulating meteoritic or metamorphic fluids at this depth, or to the physical conditions within the fault that did not permit the precipitation of graphite.

5. Conclusions

[11] The TTF is uniform in its electrical properties along-strike for more than 350 km. This homogeneity has been observed both in the raw data and in the electrical conductivity models obtained. In the upper part of the models (<5 km depth) the fault is imaged as a system of subvertical structures, suggesting that the TTF is formed by a system of faults rather than by a single fault, consistent with seismic interpretation and field mapping. At deeper levels, the presence of high conductivity anomalies ($\sim 1 \Omega \cdot \text{m}$) has been mapped in areas lateral to the surface expression of the fault. The most prominent feature of the fault zone itself is a resistive zone in the mid to lower crust below the surface trace of the fault system.

[12] **Acknowledgments.** The financial support for this project came from Lithoprobe and the Geological Survey of Canada. The broadband data were collected by Geosystem Canada. J. Spratt and G. Wennberg for collecting the long period (LIMS) MT data. D. Snyder and J. Craven provided helpful comments on this work. C. Roots, D. Murphy and all the people of the Yukon Geology Program for their assistance. The comments of two anonymous reviewers helped to improve this work. Geological Survey of Canada Contribution number 2001070. LITHOPROBE publication number #1249.

References

Abraham, A. C., D. Francis, and M. Polvé, Recent alkaline basalts as probes of the lithospheric roots of the Northern Canadian Cordillera, *Chemical Geology*, 175, 361–381, 2001.

Aleinkoff, J. N., G. L. Farmer, R. O. Rye, and W. J. Nokleberg, Isotopic evidence for the sources of Cretaceous and tertiary granitic rocks, east-central Alaska: Implications for the tectonic evolution of the Yukon-Tanana terrane, *Can. J. Earth Sci.*, 37, 945–956, 2000.

Coney, P. J., D. L. Jones, and J. W. H. Monger, Cordilleran suspect terranes, *Nature*, 288, 329–333, 1980.

Cook, F. A., et al., LITHOPROBE seismic reflection profiling of the northern Canadian Cordillera: First results of the SNORCLE profiles 2 and 3, in *SNORCLE Transect and Cordilleran Tectonics Workshop Meeting, Lithoprobe report No. 79*, compiled by F. Cook and P. Erdmer, pp. 36–49, 2001.

Clowes, R. M., et al., LITHOPROBE—New perspectives on crustal evolution, *Can. J. Earth Sci.*, 29, 1813–1864, 1992.

Geiger, H. D., and F. A. Cook, Analyses of crustal structure from bandpass

and directionally filtered potential-field data: An example from western Canada, *Can. J. Earth Sci.*, 38, 953–961, 2001.

Groom, R. W., and R. C. Bailey, Decomposition of magnetotelluric impedance tensors in the presence of local three-dimensional galvanic distortion, *J. Geophys. Res.*, 94, 1913–1925, 1989.

Ingham, M., and C. Brown, A magnetotelluric study of the Alpine Fault, New Zealand, *Geophys. J. Internat.*, 135, 542–552, 1998.

Jones, A. G., et al., Electromagnetic constraints on strike-slip fault geometry—the Fraser River fault system, *Geology*, 20, 561–564, 1992.

Lowe, C., et al., New geophysical data from the northern Cordillera: Preliminary interpretations and implications for the tectonics and deep geology, *Can. J. Earth Sci.*, 31, 891–904, 1994.

Mackie, R., D. Livelybrooks, T. Madden, and J. Larsen, A magnetotelluric investigation of the San Andreas Fault at Carrizo Plain, California, *Geophysical Research Letters*, 24(15), 1847–1850, 1997.

Mathez, E. A., et al., Electrical conductivity and carbon in metamorphic rocks of the Yukon-Tanana terrane, Alaska, *J. Geophys. Res.*, 100, 10,187–10,196, 1995.

McNeice, G., and A. G. Jones, Multisite, multifrequency tensor decomposition of magnetotelluric data, *Geophysics*, 66(1), 158–173, 2001.

Monger, J. W. H., et al., Continent–ocean transition in western North America between latitudes 46 and 54 degrees: Transects B1, B2, and B3, in *Phanerozoic evolution of North American continent-ocean transitions*, edited by R. C. Speed, Geological Society of America, Decade of North American Geology Continent–Ocean Transect Vol., pp. 357–397, 1994.

Nesbitt, B. E., and K. Muehlenbachs, Genetic implications of the association of mesothermal gold deposits with major strike-slip fault systems, in *North American conference on tectonic control of ore deposits and the vertical and horizontal extents of ore systems, Proceedings volume*, Univ. Mo., Rolla, Mo., USA, pp. 57–66, 1988.

Price, R. A., and D. M. Carmichael, Geometric test for late Cretaceous–Paleogene intracontinental transform faulting in the Canadian Cordillera, *Geology*, 14, 468–471, 1986.

Rodi, W., and R. L. Mackie, Nonlinear conjugate gradients algorithm for 2-D magnetotelluric inversion, *Geophysics*, 66, 174–187, 2001.

Snyder, D., and B. Roberts, Seismic characterization of two major tectonic zones in the Canadian Cordillera: The Teslin and Tintina zones along SNORCLE Line 3, in *SNORCLE Transect and Cordilleran Tectonics Workshop Meeting, Lithoprobe report No. 79*, compiled by F. Cook and P. Erdmer, pp. 50–53, 2001.

Stanley, W. D., et al., The Denali fault system and Alaska Range of Alaska; evidence for underplated Mesozoic flysch from magnetotelluric surveys, *Geological Society of America Bulletin*, 102(2), 160–173, 1990.

Staveley, J., B. E. Nesbitt, and K. Muehlenbachs, Geochemistry of the Ketza river mineral deposits, Pelly Mountains, Central Yukon, in *Joint annual meeting of the Geological Association of Canada and the Mineralogical Association of Canada with the Society of Economic Geologist*, 16, Geological Association of Canada, Waterloo, Ontario, Canada, p. 118, 1991.

Tempelman-Kluit, D. J., Transported cataclasisite, ophiolite, and granodiorite in Yukon: Evidence of arc-continent collision, Geological Survey of Canada Paper, 79-14, 27 pp., 1979.

Unsworth, M. J., P. E. Malin, G. D. Egbert, and J. R. Booker, Internal structure of the San Andreas Fault at Parkfield, California, *Geology*, 25, 359–362, 1997.

Unsworth, M. J., G. D. Egbert, and J. R. Booker, High-resolution electromagnetic imaging of the San Andreas Fault in Central California, *J. Geophys. Res.*, 104, 1131–1150, 1999.

Varsek, J. L., et al., LITHOPROBE crustal reflection structure of the southern Canadian Cordillera II: Coast Mountains transect, *Tectonics*, 12, 334–360, 1993.

Wannamaker, P. E., G. W. Hohmann, and S. H. Ward, Magnetotelluric responses of three-dimensional bodies in layered earths, *Geophysics*, 49, 1517–1533, 1984.

Weldford, J. K., et al., Lithospheric structure across the craton-Cordilleran transition of northeastern British Columbia, *Canadian Journal of Earth Sciences*, 38(8), 1169–1189, 2001.

Wu, X., I. J. Ferguson, and A. G. Jones, Magnetotelluric investigation of the Great Slave Lake Shear Zone on LITHOPROBE SNORCLE Transect 1A, submitted to *Earth Planet. Sci. Lett.*, 2001.

Yukon MINFILE, Exploration and Geological Services Division, Yukon, Indian and Northern Affairs Canada, 1997.

A. G. Jones and J. Ledo, Geological Survey of Canada, 615 Booth St., Ottawa, Ontario, K1A 0E9, Canada. (ajones@cg.nrcan.gc.ca; jledo@cg.nrcan.gc.ca)

I. J. Ferguson, Geological Sciences, University of Manitoba, Winnipeg Manitoba, R3T 2N2, Canada. (ij_ferguson@UManitoba.CA)